Journal of Structural Biology **127,** 141–151 (1999)
Article ID jsbi.1999.4135, available online at http://www.idealibrary.com on IDEAL®

Metal Compounds as Tools for the Construction and the Interpretation of Medium-Resolution Maps of Ribosomal Particles

Shulamith Weinstein,* Werner Jahn,† Carola Glotz,‡ Frank Schlünzen,§ Inna Levin,* Daniela Janell,§ Jörg Harms,§ Ingo Kölln,§ Harly A. S. Hansen,§ Marco Glühmann,§ William S. Bennett,§ Heike Bartels,*,§ Anat Bashan,* Ilana Agmon,* Maggie Kessler,* Marta Pioletti,‡ Horacio Avila,‡ Kostas Anagnostopoulos,‡ Moshe Peretz,* Tamar Auerbach,*,§ Francois Franceschi,‡ and Ada Yonath*,§

**Department of Structural Biology, Weizmann Institute, 76100 Rehovot, Israel; †Max-Planck-Institute for Medical Research, Jahn Strasse 29, 69120, Heidelberg, Germany; ‡Max-Planck-Institute for Molecular Genetics, Ihnestrasse 73, 14195 Berlin, Germany; and §Max-Planck-Research Unit for Ribosomal Structure, Notkestrasse 85, 22603 Hamburg, Germany*

Received January 25, 1999, and in revised form April 30, 1999

Procedures were developed exploiting organometallic clusters and coordination compounds in combination with heavy metal salts for derivatization of ribosomal crystals. These enabled the construction of multiple isomorphous replacement (MIR) and multiple isomorphous replacement combined with anomalous scattering medium-resolution electron density maps for the ribosomal particles that yield the crystals diffracting to the highest resolution, 3 Å, of the large subunit from *Haloarcula marismortui* and the small subunit from *Thermus thermophilus.* The first steps in the interpretation of the 7.3-Å MIR map of the small subunit were made with the aid of a tetrairidium cluster that was covalently attached to exposed sulfhydryls on the particle's surface prior to crystallization. The positions of these sulfhydryls were localized in difference Fourier maps that were constructed with the MIR phases.

Key Words: **ribosomes; crystallography of ribosomes; tetrairidium cluster; $Ta_6 Br_{14}$.**

INTRODUCTION

Ribosomes are the supramolecular assemblies responsible for one of the most fundamental life processes, the translation of the genetic code into proteins. The ribosomes are giant nucleoprotein organelles built of two independent subunits of unequal size that associate upon the initiation of protein biosynthesis. In bacteria their molecular mass is about 2.3 MDa and they are composed of RNA and proteins at a 2:1 ratio. The large subunit, called 50S[1] in prokaryotes, is 1.45 MDa, contains two RNA chains with a total of 3000 nucleotides, and contains 38–50 different proteins. It catalyzes the formation of the peptide bond and provides the path for the progression of nascent proteins. The small subunit, 30S, is 0.85 MDa and consists of one RNA chain of 1500 nucleotides and 21 proteins. It offers the site for the initiation and the progression of the process of protein biosynthesis and facilitates the decoding of the genetic information.

Crystals have been grown from intact prokaryotic ribosomes and their subunits. Diffraction to around 3 Å was obtained from two crystal types: the large ribosomal subunits from *Haloarcula marismortui,* H50S (von Böhlen *et al.,* 1991), and the small subunits from *Thermus thermophilus,* T30S (Yonath *et al.,* 1998; Harms *et al.,* 1999). Experience showed that the complications in the elucidation of the high-resolution structure of the ribosome are linked not only to the huge size of the ribosomes and to the lack of internal symmetry. They stem primarily from the inherent flexibility and high instability of the ribosomes, since their surface is composed of highly degradable RNA alongside proteins that may be loosely held. These undesired properties are accom-

[1] Abbreviations used: 70S, 50S, 30S: the whole ribosome and its two subunits from prokaryotes. A letter as a prefix to the ribosomal particles or ribosomal proteins represents the bacterial source (e.g., E, *E. coli;* T, *Thermus thermophilus;* H, *Haloarcula marismortui*). tRNA and rRNA: transfer and ribosomal RNA. The names of the ribosomal proteins are composed of L or S (showing that this protein is of the large or small subunit) and a running number, according to the position of this protein on the two-dimensional gels. SR: synchrotron radiation; MIR: multiple isomorphous replacement; MIRAS and SIRAS: multiple and single isomorphous replacement combined with anomalous scattering; MAD: multiwavelength anomalous dispersion; MR: molecular replacement. The chemical formulae of the undecagold and the tetrairidium clusters (including their reactive bridging arms), as well as those of TAMM, PIP, WAC, Hg_6, Hg_3, W12, W17CsCo, W18, and W30, are given in Table I.

1047-8477/99 $30.00

panied by severe radiation sensitivity of the ribosomal crystals, observed even at cryo-temperature when using the bright SR beam required for high-resolution data collection (Krumbholz *et al.,* 1998) and often also by an extremely low level of isomorphism, fluctuations in the unit cell dimensions, deformed spot-shape, and nonisotropic mosaicity. Owing to these problems, the assignment of phases is being performed in a progressive fashion, from low to higher resolution, and it is important that each step is supported and validated by several independent approaches.

The commonly used methods for phasing diffraction data from crystals of biological macromolecules are the multiple and single isomorphous replacement (MIR and SIR) and their combination with anomalous diffraction (MIRAS and SIRAS, respectively). These, as well as MAD, require the preparation of heavy atom derivatives, usually by introducing electron-dense atoms to the crystalline lattice at distinct locations. The added atoms should be dense enough to create measurable changes in the diffraction amplitudes, while keeping the crystal structure isomorphous with that of the native molecule. Derivatization of crystals of biological macromolecules is routinely obtained by their soaking in solutions of heavy atom compounds, assuming that the high affinity of the metal compound to specific exposed side chains will lead to selective attachment with a high yield. Using this equilibrium procedure, productive derivatization in one or a few sites is largely a matter of chance, but in most cases was found to lead to useful derivatives.

As the changes in the structure factor amplitudes resulting from the addition of the heavy atoms are being exploited, the derivatization reagents are chosen according to their potential ability to induce measurable signals. Single heavy atom compounds yielded useful high-resolution phases for several large macromolecules assemblies. Among these are viruses that contain a very high internal symmetry (e.g., Yan *et al.,* 1995; Rossmann, 1995; Hogle *et al.,* 1985; Basak *et al.,* 1997) and several macromolecules of lower internal symmetry, such as the 371 kDa ATPase (Abrahams and Leslie, 1996), the 840 kDa GroE1 (Braig *et al.,* 1994), and the 250 kDa $tRNA^{phe}$ synthetase and its complex with its cognate tRNA (Goldgur *et al.,* 1997). Somewhat larger heavy atom compounds, such as TAMM and PIP (Table I), were the key for phasing the data obtained from the nucleosome-core particle (O'Halloran *et al.,* 1987; Luger *et al.,* 1997), the photosynthetic reaction center (Deisenhofer *et al.,* 1984), an idiotope–anti-idiotype complex (Bentley *et al.,* 1990), and glutathione transferase (Reinemer *et al.,* 1991). Another medium-size material, Ta_6Br_{14} (Harder and Preetz, 1990), was found to be useful for structure determination at 1.8 to 5.5-Å resolution (summarized by Knäblein *et al.,* 1997; Neuefeind *et al.,* 1997). Examples are a recombinant immunoglobulin domain (Stepie *et al.,* 1992), transketolase (Schneider and Lindqvist, 1994), the 550- kDa ribulose-1,5-phosphate carboxylase/oxygenase (Andersson *et al.,* 1989), the 250-kDa GTP-cyclohydrolase (Nar *et al.,* 1995), and the 673-kDa proteosome at 3.4 Å (Löwe *et al.,* 1995).

Crystals diffracting to 3-Å resolution were obtained by us from the large ribosomal subunits from *H. marismortui,* H50S, and from the small subunit from *T. thermophilus,* T30S. Exploiting the combination of heavy atom compounds of different sizes, from monocation salts to multimetal clusters, led to successful derivatization of the T30S crystals to 3.6-Å resolution and of H50S up to about 5-Å resolution. To validate the main features of the expected structures, we constructed MIR and its combination with anomalous signal, MIRAS electron density maps, to 7.2 and 8.5 Å, respectively (Yonath *et al.,* 1998; Harms *et al.,* 1999). Below we discuss these maps, focusing on the specific contributions of various heavy atom compounds used by us.

TABLE I
Metal Compounds

PIP, di-iododiplatinum (II) diethyleneamine[a]
TAMM, tetrakis(acetoxymercuri)-methane
WAC, $W_3O_2(acetate)_6(H_2O)_3CF_3SO_3$
Hg3, $Hg_3C_6O_4H_8$[a]
Ta_6Cl_{14}
$Ta_6Br_{14} \cdot 2H_2O$[a]
Nb_6Cl_{14}
Hg6, $C_2Hg_6N_2O_8$[a]
$Ir_4(CO)_8R'_3R''''$; $Ir_4(CO)_8R''_4$; $Ir_4(CO)_8R'_3R''$ [a,b]
$Au_{11}P'_6P''(CN)_3$ [a,b]
W11Rh, $Cs_5H_xSiW_{11}O_{39}Rh^{III}$ $CH_3COO(H)$[b]
W17-Th, $Cs_7(P_2W_{17}O_{61}Th(NC_5H_5))nH_2O$[b]
W30, $K_{14}(NaP_5W_{30}O_{110})31H_2O$
W12(K), $K_5H(PW_{12}O_{40})12H_2O$ [a]
W18, $(NH_4)_6(P_2W_{18}O_{62})14H_2O$[a]
W17CsCo, $Cs_7(P_2W_{17}O_{61}Co(NC_5H_5))14H_2O$[a]
W17LiCo, $Li_7(P_2W_{17}O_{61}Co(NC_5H_5))14H_2O$
BuSnW17, $K_7[(buSn)(P_2W_{17}O_{61})]10H_2O$
PhSnW15, $K_5H_4[(phSn)_3(P_2W_{15}O_{59})]16H_2O$
BuSnW15, $K_5H_4((buSn)_3(P_2W_{15}O_{59})]15H_2O$
W12(Na), $Na_{16}[(O_3PCH_2PO_3)_4W_{12}O_{36}]40H_2O$

R′ = $P(CH_2CH_2CONH_2)_3$; R″ = $P(CH_2CH_2CONH_2)_2(CH_2CH_2CONHCH_2CH_2NH_2)$[c]
R‴ = $P(CH_2CH_2COOH)_3$; R⁗ = $P(CH_2CH_2CONHCH_2CH_2N(CH_3)_2)_3$
P′ = $P(C_6H_4CH_2N(COCH_3)CH_2CH_2OH)_3$; P″ = $P(C_6H_5)_2C_6H_4CH_2NH_2$[c]

Note. bu, butyl; ph, phenyl.
[a] Found useful for phasing or for map interpretation.
[b] Designed for covalent binding.
[c] The activation was via the primary amino group.

Owing to the complexity of the ribosomal structure, means for independent map interpretations are being developed. In this article we present studies on covalently derivatized T30S particles by a medium-size cluster, tetrairidium. Prepared as a monofunctional sulfhydryl reagent, this cluster was bound to free -SH moieties on the surface of ribosomal particles. The crystals of the modified T30S subunits were found to be isomorphous with the native ones and led to well-behaving data to 4.5 Å. Using the currently available MIR phases (Harms *et al.,* 1999), difference Fourier analysis revealed the positions of the bound clusters. Hence, the locations of the surfaces of the proteins to which the cluster was bound, namely TS11 and TS13, have been determined.

USEFUL HEAVY ATOMS IN RIBOSOMAL CRYSTALLOGRAPHY

In contrast to the availability of numerous single heavy atom materials, there are only a few stable water-soluble polyheavy atom compounds (Table I; and Thygesen *et al.,* 1996). In the ideal case these materials should consist of a large number of heavy atoms, linked directly to one another in the most compact fashion. Examples are monofunctional reagents of dense metal clusters, designed for covalent binding at specific sites, and compounds that may be employed for soaking experiments such as charged clusters, heteropolyanions, and soluble multicoordination compounds. In soaking experiments, the large size of these compounds may be advantageous as it should eliminate multiple site binding, but on the other hand, it may hamper their penetration into the crystals. Nevertheless, several heteropolytungstate anions (e.g., Dawson, 1953; Brown *et al.,* 1977; Alizadeh *et al.,* 1985; Xin and Pope, 1994; Wei *et al.,* 1997) that possess a high degree of internal symmetry yielded structures at relatively high resolution for riboflavin synthase at 3.3 Å (Ladenstein *et al.,* 1987), fumarase C at 2.6 Å (Weaver *et al.,* 1994), and the proteosome at 3.4 Å (Löwe *et al.,* 1995).

Ta_6Br_{14} was found to be the strongest heavy atom among those that led to the construction of the electron density maps of all three crystal forms studied by us, T50S, H50S, and T30S (Yonath and Franceschi, 1998; Yonath *et al.,* 1998). An additional medium-size compound that yielded phase information is $C_2Hg_6N_2O_8$ (called here Hg_6), a compound that was synthesized first almost 100 years ago (Hofmann, 1900). In contrast, TAMM, the key compound in structure determination of several large biological assemblies (for references see Introduction), could not be used for soaking the ribosomal crystals, either because of its limited solubility in the saline solution of H50S or because it caused dramatic changes in cell dimensions of T30S (from 167 to 173 Å) and often also a significant increase in the mosaicity of these crystals.

Quantitative covalent binding of a heavy atom compound at predetermined sites prior to crystallization is an alternative for derivatization by soaking. This approach requires complicated and time-consuming procedures, but is expected to yield information about the localizations of the ribosomal components to which the heavy atoms are bound, which may be indispensable at the more advanced stages in the course of structure determination. The feasibility of this approach has been recently proven at 2.8 Å for another large cell organelle, the nucleosome-core particle (Luger *et al.,* 1997). However, the procedure developed for the latter, i.e., producing a recombinant nucleosome from its individual components into which binding sites were introduced genetically, cannot be fully adopted for high-resolution phasing of ribosomes, since so far all *in vitro* reconstituted ribosomal particles studied by us, namely, T30S, H50S, B50S, T70S, and T50S (Berkovitch-Yellin *et al.,* 1992), did not yield well-diffracting crystals, although they display high functional activity. Therefore our strategy is to attach the heavy atom compounds to exposed chemically active moieties on the surface of the ribosomes or on materials that bind to ribosomes with a high affinity and selectivity, such as antibiotics.

Undecagold and tetrairidium clusters (Jahn, 1989a,b), in which the heavy metal cores are surrounded by chemical "envelopes" that contain features frequently observed in proteins, designed to increase their solubility and stability, are being used for this aim. These clusters were prepared as monofunctional reagents with a chemically reactive arm that can bind to selected moieties, such as sulfhydryls or primary amines (Weinstein *et al.,* 1989, 1992). The undecagold cluster was found to be suitable only for low-resolution studies (Bartels *et al.,* 1995), since its core is of a diameter of 8.2 Å and since its chemical envelopes possesses limited internal symmetry. Consequently, its monofunctional reactive arm may be any one of 21 potential binding sites, belonging to three different symmetrically groups, among which none possesses special properties that may direct specific binding to the macromolecular target.

The tetrairidium cluster is similar to, albeit significantly smaller (core of a diameter of 4.8 Å) and more symmetrical than, the undecagold cluster. Hence its phasing power may extend to almost atomic resolution. In order to maximize the rigidity and minimize the free movement of its bridging arm, we designed it with a length slightly longer than the of lysine's side chain and with an amide bond in the middle of it (R″

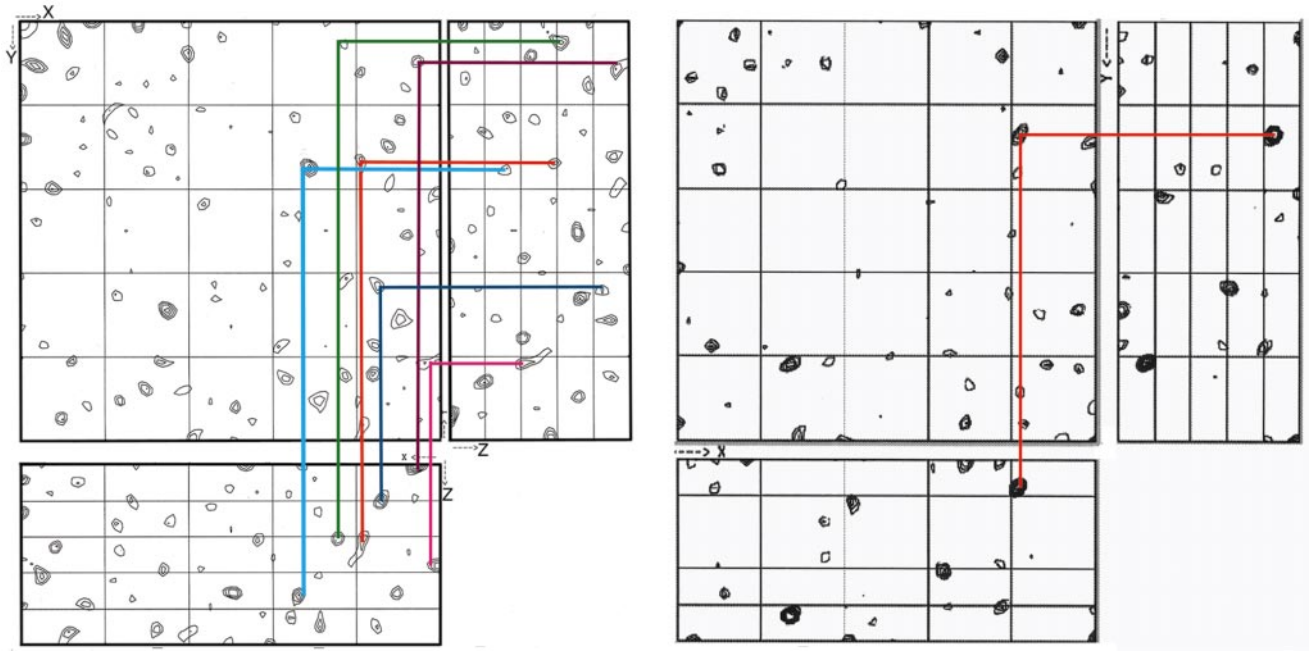

FIG. 1. (Left) Harker sections of difference Patterson maps of T30S constructed at 6.4 Å. Derivatization was performed with a trimetal salt (Pb_3citrate). A typical example for a rather flat, albeit overcrowded map. (Right) Harker sections from a readily interpretable difference Patterson map of T30S constructed at 9-Å resolution. Derivatization was performed by a multi-W cluster (electron density of 2.6 electrons/Å^3). This map represents an exceptional case.

in Table I). So far we used maleimido as an SH reagent despite its potential chirality, because we could optimize its binding to the ribosome. In contrast, the optimization of the binding of the cluster to which nonchiral hands (e.g., made from iodo- or bromo-acetate) were attached met with considerable difficulties.

Attempts to exploit the tetrairidium and the undecagold clusters as soaking reagents were also made. In order to increase their suitability, they were prepared either as monofunctional reagents that were chemically activated shortly before soaking or as charged compounds. Examples are a tetrairidium cluster with three basic groups or with 12 acidic groups (see also Table I).

THE SMALL RIBOSOMAL SUBUNIT

The T30S crystals diffract to 3-Å resolution and exhibit reasonable isomorphism (Yonath *et al.,* 1998; Harms *et al.,* 1999). Consequently, despite their high radiation sensitivity, complete data sets could be constructed from native and derivatized crystals by irradiating narrow regions of the crystals separately. Most of the heavy atom compounds used for derivatization (ranging from Ta_6Br_{14} and Hg_6 to monometal compounds) led to multisite binding that resulted in overcrowded and rather flat difference Patterson maps (Fig. 1). These, in turn, imposed the need for extensive cross-verifications with Fourier methods.

This 7.2-Å MIR map shows features of size and shape consistent with those assigned for T30S within the cryo-EM reconstruction of T70S (Stark *et al.,* 1995; Frank *et al.,* 1995; Gabashvili *et al.,* 1999; Harms *et al.,* 1999). These contain globular regions of density appropriate in size and shape for ribosomal proteins as well as elongated continuous dense features of a shape similar to that observed in the maps of the nucleosome core particle at comparable resolution (Richmond *et al.,* 1984). The latter span the particle at various directions and could be traced as double- and single-stranded rRNA chains (Harms *et al.,* 1999).

FIG. 2. The locations of the two bound tetrairidium clusters in the 7.2-Å MIR map of T30S. The binding sites are shown as yellow squares, highlighted by arrows on one particle (one asymmetric unit). For clarity, the same map on which the cryo-EM reconstructed model of T30S (Harms *et al.,* 1999) is superimposed is shown at the bottom. 20 688 reflections in the range of 7.2–30 Å were included and 46 sites of four derivatives were refined by MLPHARE yielding R_{sym} = 8.6–14.2%, completeness = 84–99%, R_{scale} (to native) = 21–29%, FOM = 0.671, phasing power up to 1.4, R_{cullis} = 0.8–0.91. The MIR map was subjected to density modification assuming 65% solvent (for more detail see Harms *et al.,* 1999).

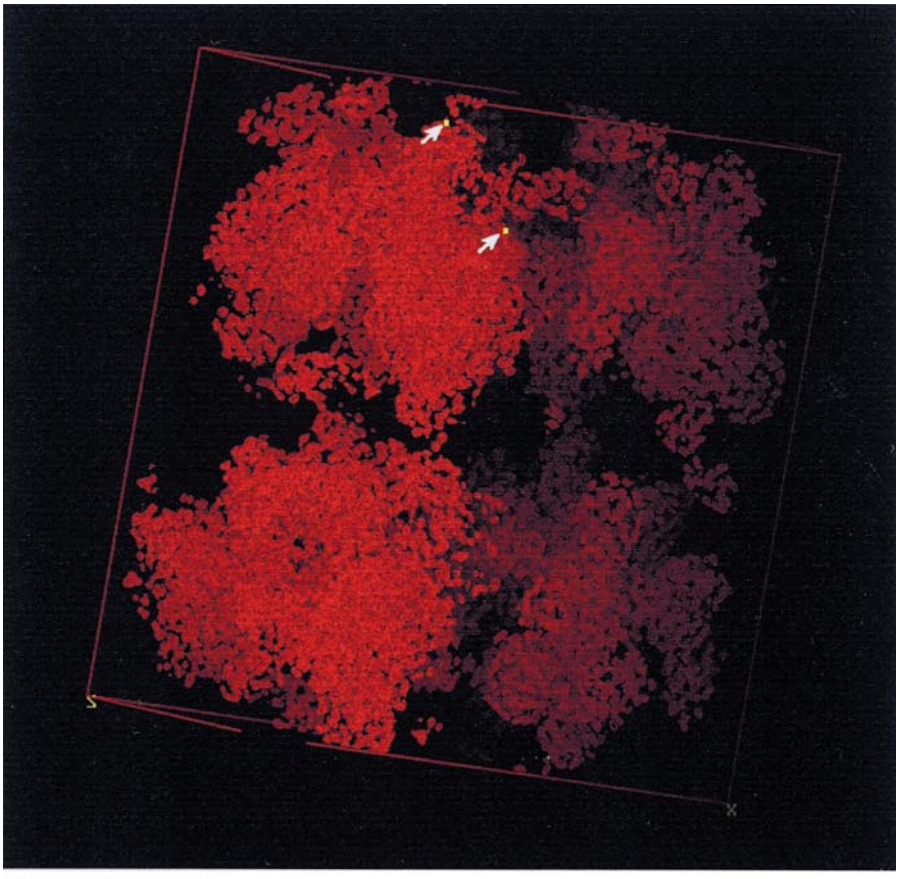

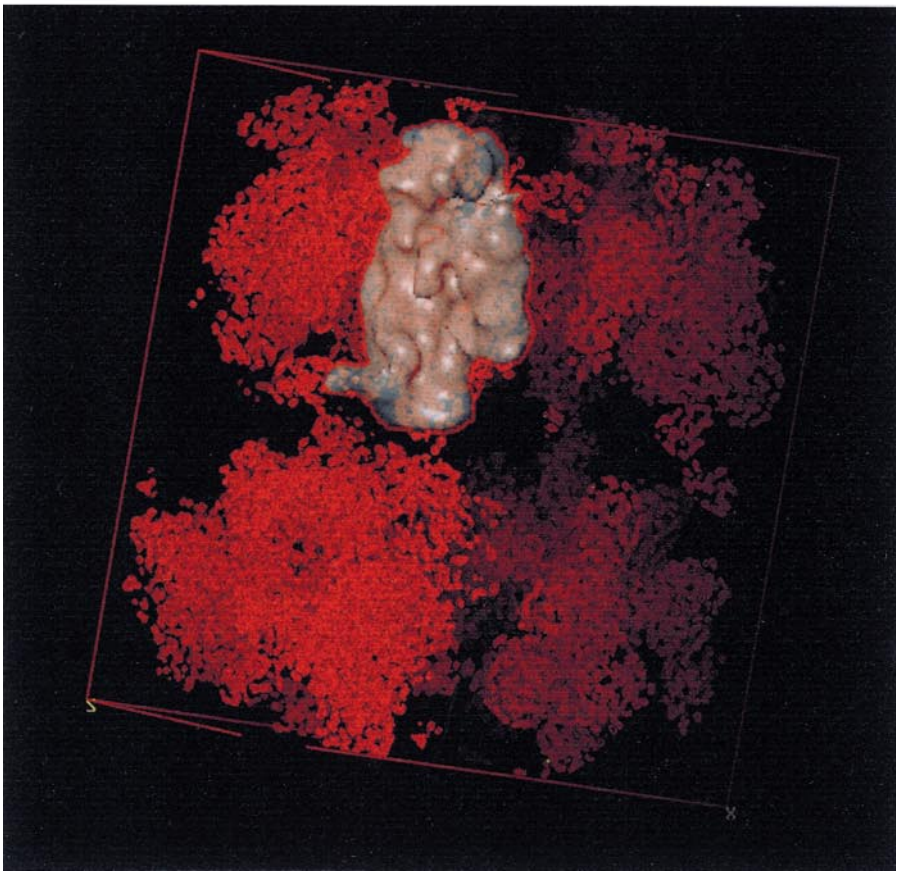

As mentioned above, in order to enable reliable assignments of the various components of T30S, we are exploiting the monofunctional reagent of the tetrairidium cluster (Jahn, 1989b). As all ribosomal particles contain only a few exposed SH groups, these are being used for cluster binding. Labeling studies showed one fully exposed and one partially exposed SH group (Sagi *et al.,* 1995), belonging to proteins TS11 and TS13 (Wada *et al.,* 1999). The crystals obtained from the so-modified particles diffract to 4.5-Å resolution and are isomorphous with the native ones. As expected, the attachment of approximately one or two equivalents of the tetrairidium cluster created a rather weak derivative for independent phasing. Thus, the 55 800 measured reflections yielded quality data (completeness of 90%, R_{sym} of 12%) but a low signal (R_{scale} to native of 19%). However, this cluster was found to be a powerful marker in the MIR electron density map of T30S. The data collected from the derivatized crystals were used together with the previously determined MIR phases (Harms *et al.,* 1999) for the construction of a difference Fourier map. Thus, two prominent peaks were revealed in this map, both with noise to background signals of 2.5 and 4.5 σ (the highest in the map). Incidently, corresponding peaks were also detected in difference Patterson maps, but these exhibited limited phasing power once exposed to refinement (e.g., their final FOM was 0.3).

Based on the high level of clarity at which the sites assigned to the iridium cluster were observed, it seems that although the arm bridging between the clusters' core and the SH group contains inherent flexibility, the crystallization of the modified T30S particles limited its motion, as frequently happens to long side chains in proteins. Interestingly, no clear separation between the features belonging to T30S and the bridging arm was observed in the electron density maps constructed with the data collected from the tetrairidium-bound crystals, since the chemical nature of the arm (R″ in Table I) is very similar to that of proteins.

The site of the major iridium cluster is located at the central part of the particle, not far from the part called the "neck" of the small ribosomal subunits (Stark *et al.,* 1995; Frank *et al.,* 1995; Gabashvili *et al.,* 1999). This location is roughly compatible with that suggested by immunoelectron microscopy for protein S11 in *Escherichia coli* 30S (Stöffler and Stöffler-Meilicke, 1986). It is also rather close to the position suggested in recent assignments of ribosomal components within cryo-EM reconstructions (Mueller and Brimacombe, 1997). However, it deviates by approximately 35 Å from the position assigned to the center of mass of this protein by triangulation, a method exploiting neutron scattering and the variations in the contrasts of protonated and deuterated ribosomal components (Moore *et al.,* 1985). Such deviation is tolerable since the tetrairidium cluster and the immunoelectron microscopy target the external surface of the particles, whereas the triangulation method approximates the positions of the centers of mass of the r proteins and bears uncertainties about their shapes (elongated, spherical, etc.). Furthermore, the discrepancy found by us is smaller than the inconsistencies of 65 Å between the neutron scattering triangulation studies and those exploiting complementary DNA for the localization of ribosomal components (Alexander *et al.,* 1994).

The minor Ir site is located in the middle of the particle's "head" (Fig. 2). It corresponds to the sulfhydryl of protein TS13 (Wada *et al.,* 1999). According to the results of SH labeling experiments, this site is its only partially exposed end. This may explain its appearance with a lower height in the difference Fourier map (2.5 σ vs 4.5 σ of that assigned to be bound to TS11), although we assume high homogeneity within the crystal. The location of this peak was readily determined and found to be in agreement with that of TS13, as determined by all the above-mentioned approaches (Moore *et al.,* 1985; Stöffler and Stöffler-Meilicke, 1986; Mueller and Brimacombe, 1997).

THE LARGE RIBOSOMAL SUBUNIT

Three-dimensional crystals were obtained from large ribosomal subunits from several bacterial sources (Berkovitch-Yellin *et al.,* 1992), among them two (of T50S and H50S) that seem to be suitable for crystallographic studies. These crystals of T50S were vastly improved most recently, as strong diffraction to 3.6 Å was observed (F. Franceschi, J. Muessig, and D. Janell, to be published). Until recently the crystals of this subunit led to high-quality diffraction data but only to low resolution, 9–10 Å (Volkmann *et al.,* 1990).

The crystals of H50S diffract to over 2.7 Å (von Böhlen *et al.,* 1991). However, owing to the undesirable properties of the crystals of H50S, despite the intensive studies carried out by us (Yonath and Franceschi, 1998; Yonath *et al.,* 1998) as well as by others (Ban *et al.,* 1998), so far electron density maps of H50S have been constructed only to 8 to 9-Å resolution.

It was found that the very large metal compounds used for soaking or precrystallization covalent binding led to the phasing only in association with additional structural information, such as cryo-EM reconstructions (Ban *et al.,* 1998; Harms *et al.,* 1999). The smaller heavy atom compound, Ta_6Br_{14}, was found to be much more powerful in phasing presum-

ably because its small size permits penetration into crowded regions, thus becoming tightly bound (Fig. 3). Furthermore, the most occupied Ta_6Br_{14} isomorphous sites of H50S were detected in difference Patterson maps up to about 5-Å resolution (Fig. 3), a range at which the contributions of the other three compounds (W12, W17CsCo, W30) used for constructing the 10- to 12-Å resolution MIRAS map became very low. It should also be mentioned that the major Ta_6Br_{14} sites were detected in the difference Fourier maps constructed with phases obtained by molecular replacement studies, using cryo-EM reconstructions (Yonath and Franceschi, 1998; Harms *et al.,* 1999). Interestingly, another research group, attempting to phase data obtained from identical H50S crystals, found Ta_6Br_{14} to be the weakest heavy atom compound (Ban *et al.,* 1998).

The packing scheme of the crystals of H50S (Fig. 3) may shed light on the odd combination of high resolution and otherwise poor diffraction. Part of the unit cell is closely packed, whereas the *c* axis (of 564 Å) is loosely held by a narrow contact region surrounded by a very large continuous solvent volume. The close packing may be connected to the high resolution, 2.7 Å, whereas the limited size of the loose contact region that permits only a small number of interparticle interactions may be the cause of the low level of isomorphism, the unusual morphology (very thin plates reaching typically up to 0.5 mm^2 with an average thickness of a few micrometers in the direction of the *c* axis), and the variations in the length of the *c* axis (from the average length of 564 Å to the extreme of 580 Å) caused by the irradiation (Yonath *et al.,* 1998).

The ability of the very large clusters to readily diffuse into the H50S crystals may also be explained by the special packing arrangement of this system. It is conceivable that the large clusters that diffused into the sizable solvent body maintain some free movement, thus introducing subtle nonisomorphism that may not be detected as such in routinely treated diffraction data, leading to limited or less reliable phasing information (Schlünzen *et al.,* 1995). Indeed, only three to six cluster sites were detected in difference Patterson maps, by us (Schlünzen *et al.,* 1995; Yonath *et al.,* 1998) as well as by others (Ban *et al.,* 1998), whereas 18–20 equivalents of W30 clusters per ribosomal particle were detected using atomic absorption in dissolved ribosomal crystals that had been previously soaked in solutions containing millimolar amounts of heteropolytungstates for 10 h and then thoroughly washed, 24 times within 42 h (Yonath *et al.,* 1998). Simulation studies indicated that such large amounts of "floating" tungsten clusters are sufficient to generate measurable anomalous signals at low resolution and may mislead the process of phasing.

CONCLUSIONS AND PROSPECTIVE

We have shown that low- and medium-resolution MIR and MIRAS maps can be constructed for ribosomal particles and that selected locations on them can be revealed by covalently bound medium-size heavy atom compounds, such as a tetrairidium cluster. All the heavy atom compounds used by us may be suitable for MAD phasing as their fluorescence curves fall within the usable SR energies. Among them, Ta_6Br_{14} may be an attractive compound, as it contains two different moieties, each with a significant anomalous signal. The MAD experimental requirements are very demanding as the anomalous signals are significantly lower than those obtained per heavy atom with MIR. Hence, quantitative binding is desired and special concern is given for the optimization of the extent and the accuracy of the precrystallization covalent binding of reactive clusters to the ribosomal particles.

PROCEDURES

Crystal Growth, X-Ray Data Collection, and MIR Phasing

The crystals of H50S, T30S, and T20S were grown under conditions described previously (von Böhlen *et al.,* 1991; Yonath *et al.,* 1988; Volkmann *et al.,* 1990), with some modifications. Data were collected with SR at cryo-temperature, according to the procedures described in Berkovitch-Yellin *et al.* (1994) and processed by DENZO and SCALEPACK (Otwinowski, 1993). The electron density maps were examined using the program O (Jones *et al.,* 1991).

The data from native and Ta_6Br_{14} soaked crystals of T50S were collected to 10 Å at several wavelengths at BW7b/EMBL/DESY. These were used for constructing two SIRAS difference Patterson maps, from which the common sites were extracted and refined.

The data from native and soaked crystals of H50S were collected at BW6 and BW7b at DESY, at F1/CHESs, at BL26 PF/KEK, and at ID2/ESRF. The sites of four derivatives, among them Ta_6 Br_{14} and three tungsten clusters, were used for phasing. The positioning of the heavy atom sites was performed by a combination of difference Patterson and Fourier methods, based on the major position of Ta_6Br_{14}, found to be stable and consistent in all resolution ranges up to 5 Å. Each heavy atom position was cross-verified and refined by MLPHARE with maximum likelihood (CCP4, 1994). Since it was found that the contribution of the three tungsten clusters to the phasing process was negligible beyond 10 Å,

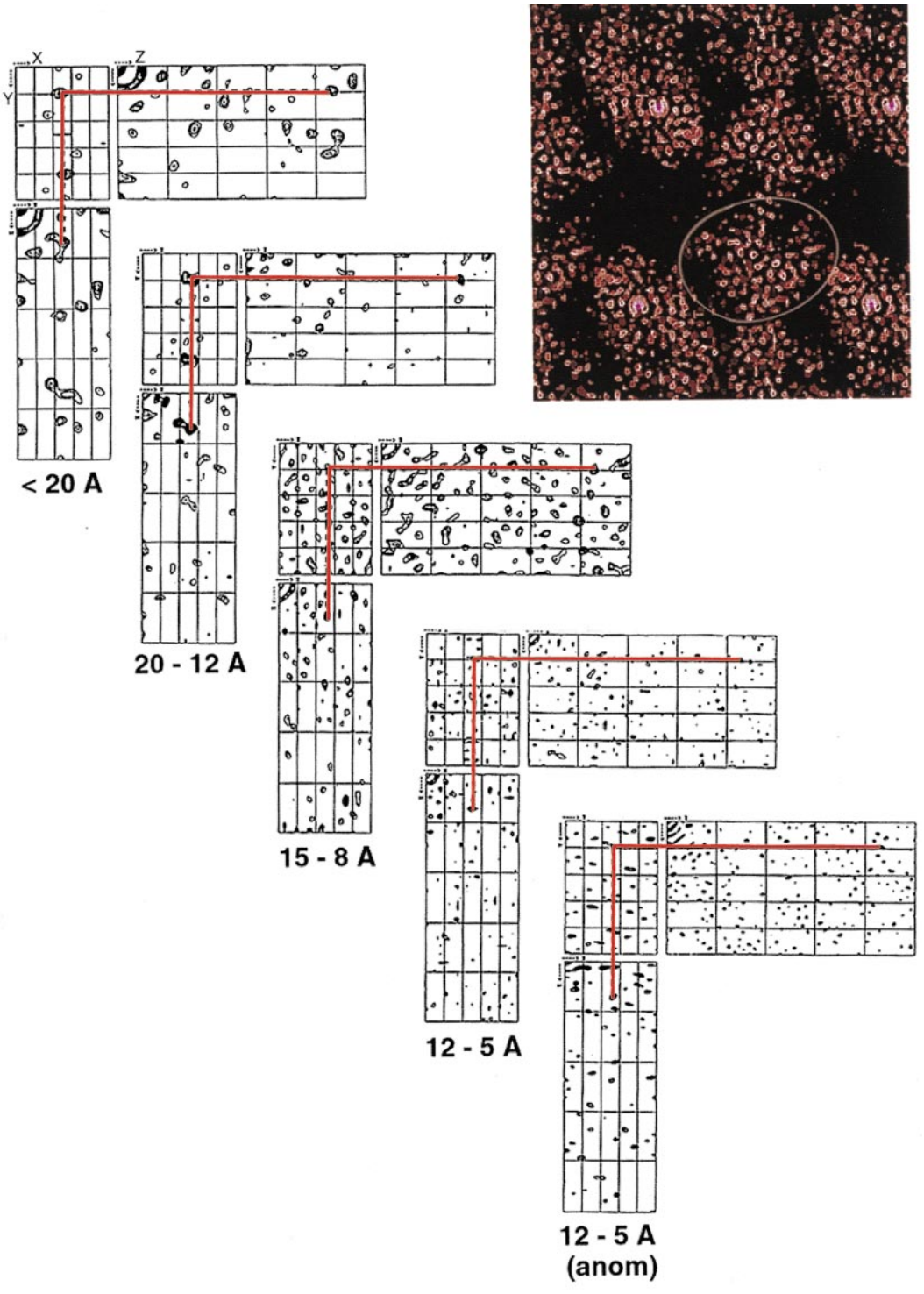

FIG. 3. A series of Harker sections of Ta_6Br_{14} difference Patterson map of H50S, displayed at different resolution ranges. (Top right) A slab of about 25 Å of the 10- to 12-Å MIR map of H50S (211 × 300 × 567 Å, $C222_1$), showing the packing arrangement of this crystal form: compact packing regions around $z = 1/4$ and 3/4 and a very small contact region at $z = 1/2$. For clarity, two unit cells are shown along the Y direction (horizontal). The ellipse shows the region corresponding to one ribosomal subunit. The dense areas at the interfaces between particles represent the position of the most occupied Ta_6Br_{14} site, with significantly enlarged size. More than 11 000 reflections were measured, and a total of 15 heavy atom sites of the three derivatives (Ta_6Br_{14}; W12 and W17CsCo) were included. The positioning of the heavy atom sites was performed by a combination of difference Patterson and Fourier methods, based on the major position of Ta_6Br_{14}, found to be stable and consistent in all resolution ranges up to 5.5 Å. Each heavy atom position was cross-verified and refined by MLPHARE with maximum likelihood. Since the contribution of the two W clusters was negligible beyond 10 Å, their scattering curve could be approximated by spherical averages of their corresponding radii (W17CsCo = 10 Å and W12 = 8–9 Å). The Ta_6Br_{14}, however, was treated as in Knablein *et al.,* (1997), owing to its potential to the higher resolution shells. Mean FOM: 0.32–0.57; R_{cullis}: 0.76–0.97; phasing power: 0.98–1.15. The map was solvent flattened: one cycle, assuming 54% solvent (Yonath *et al.,* 1998).

their scattering curve could be approximated by spherical averages of their corresponding radii (W30 = 12.5 Å, W18 = 10 Å, and W12 = 8–9 Å). The Ta_6Br_{14}, however, was treated as in Knäblein *et al.* (1997), owing to its potential to phase at higher resolution shells.

The data from T30S and its derivatized crystals were collected at BW6 and BW7b/DESY, F1/CHESS, ID2/ESRF, and ID19/APS. Four heavy atom derivatives were obtained by soaking crystals in solutions of metal compounds of varying sizes. The heavy atom positions were determined and verified by difference Patterson and difference Fourier procedures. Each heavy atom position was cross-verified. Refinement was carried out by MLPHARE with maximum likelihood.

The Synthesis of Acidic and Basic Tetrairidium Clusters

The acidic cluster was prepared employing the procedure used for producing the tetrairidium cluster dodecaamide (Jahn, 1989b), but with trimethylsilylester of tris-(2-carboxyethyl) phosphine instead of tris-(2-carbethoxyethyl) phosphine. The desilylated product was purified by ion-exchange chromatography and isolated as a triethylammonium salt.

The basic cluster was prepared by the method described by Ros *et al.* (1986), starting from an anionic tetrairidium cluster. The tris-(2-dimethylaminoethylamide) of the tris-(2-carboxyethyl) phosphine was introduced as a ligand first, followed by treatment of the monosubstituted product with tris-(2-carboxamidoethyl)phosphine to get a basic cluster with four hydrophilic ligands. The dimethylaminoethylamide groups were introduced to tris-(2-carboxymethyl)phosphine after activation with carbonyldiimidazole. The tris-(2-carboxamidoethyl) phosphine was prepared by treatment of tris-(2-carbethoxyethyl) phosphine with methanolic ammonia.

Preparation and Binding of the Monofunctional Reagent of the Tetrairidium Cluster

For soaking experiments, the reactive tetrairidium cluster was prepared with one primary amino group. A linking arm for its specific binding to SH groups was attached to its amino group, using β-maleimidopropionic acid-*N*-hydroxysuccinimide ester, as described in Jahn (1989b). Freshly prepared activated monofunctional clusters were diffused into the crystals by soaking. For precrystallization covalent binding, the free motion of the linking arm was minimized using *N*-methoxy carbonyl maleimide as a shorter linker. The binding procedure was similar to that described above for the longer linker, except for the last step of the separation of the modified ribosomes from the reaction mixture, which was performed with a sucrose cushion at 40 000 rpm at 4°C. In order to eliminate binding of the activated cluster to amino groups on the ribosomal particles, the reaction was carried out at pH 6.0.

The Identification of the Protein to Which the IR Cluster is Bound

Free sulfhydryl groups, exposed on the surface of the ribosomal particles, were detected by their reaction with radioactive SH reagents, such as *N*-ethyl-maleimide, parachloro-mercurobenzoate, and iodoacetamide, followed by polyacrylamide gel electrophoresis of the ribosomal proteins, as described in Weinstein *et al.* (1989). In the case of T30S, the amount of radioactivity detected on the particle corresponded to about one and a half equivalents and appeared in the spot occupied by TS11 (one equivalent) and TS13 (half of the previous site). As each of these proteins contains a single cysteine, we concluded that the cysteine of TS11 is fully exposed, whereas that of TS13 is partially inaccessible.

Thanks are given to W. Preetz and M. Pope for their generous gifts of heavy atom compounds, to M. Safro for active participation in phasing, to M. Eisenstein for predicting the conformational elements of TS11 and TS9, and to C. Radzwill, H. Burmeister, R. Albrecht, J. Müssig, C. Paulke, M. Laschever, S. Meier, Y. Halfon, and K. Knaack, for their excellent contributions in the different stages of these studies. Data were collected at the EMBL and MPG beam lines at DESY; F1/CHESS, Cornell University, ID2, ID13, D2AM/ESRF, Grenoble, and BL26/PF/KEK, Japan, and ID19/APS. Support was provided by the Max-Planck Society, the U.S. National Institute of Health (NIH GM 34360), the German Ministry for Science and Technology (BMBF 05-641EA), and the Kimmelmann Center for Macromolecular Assembly at the Weizmann Institute, A.Y. holds the Martin S. Kimmel Professorial Chair.

REFERENCES

Abrahams, J. P., and Leslie, A. G. W. (1996) Methods used in the structure determination of bovine mitochondrial F^1 ATPase, *Acta Crystallogr. Sept. D* **52,** 30–42.

Alexander, R. W., Muralikrishna, P., and Cooperman, B. S. (1994) Ribosomal components neighboring the conserved 518–533 loop of 16S rRNA in 30S subunits, *Biochemistry* **33,** 12109–12118.

Alizadeh, M. H., Harmalker, S. P., Jeannin, Y., Martin-Frere, J., and Pope, M. T. (1985) A heteropolyanion with fivefold molecular symmetry that contains a nonlabile encapsulated sodium ion. The structure and the chemistry of $(NaP_5W_{30}O_{110})^{-14}$, *J. Am. Chem. Soc.* **107,** 2662–2669.

Andersson, I., Knight, S., Schneider, G., Lindqvist, Y., Lindqvist, T., Branden, C-I., and Lorimer, G. (1989) Crystal structure of the active site of riboluse-bisphosphate carboxylase, *Nature* **337,** 229–232.

Ban, N., Freeborn, B., Nissen, P., Penczek, P., Graussucci, R. A., Sweet, R., Frank, F., Moore, P., and Steitz, T. (1998) The 9 Å resolution X-ray crystallography map of the large ribosomal subunits, *Cell* **93,** 1105–1115.

Bartels, H., Bennett, W. S., Hansen, H. A. S., Eisenstein, M., Weinstein, S., Müssig, J., Volkmann, N., Schlünzen, F., Agmon, I., Franceschi, F., and Yonath, A. (1995) The suitability of a mono functional reagent of an undecagold cluster for phasing

data collected from the large ribosomal subunit from *Bacillus stearothermophilus, J. Peptide Sci.* **37,** 411–419.

Basak, A. K., Grimes, J. M., Gouet, P., Roy, P., and Staut, D. I. (1997) Structures of orbivirus VP7: Implications for the role of this protein in the viral life cycle, *Structure* **5,** 871–883.

Bentley, G. A., Boulot, G., Riottot, M. M., and Poljak, R. J. (1990) Three-dimensional structure of an idiotype anti-idiotypecomplex, *Nature* **348,** 254–257.

Berkovitch-Yellin, Z., Bennett, W. S., and Yonath, A. (1992) Aspects in structural studies on ribosomes, *CRC Rev. Biochem. Mol. Biol.* **27,** 403–444.

Berkovitch-Yellin, Z., Hansen, H. A. S., Weinstein, S., Eisenstein, M., von Böhlen, K., Agmon, I., Evers, U., Thygesen, J., Volkmann, N., Bartels, H., Schlünzen, F., Zaytzev-Bashan, A., Sharon, R., Levine, I., Dribin, A., Kryger, G., Bennett, W. S., Franceschi, F., and Yonath, A. (1994) *In* Cryo-crystallography of native and derivatized ribosomal crystals, *in* Chance, B., *et al.* (Eds.), Synchrotron Radiation in Biosciences pp. 61–69, Clarendon, London.

Braig, K., Otwinowski, Z., Hedge, R., Boisvert, D. C., Joachimiak, A., Horwich, A. L., and Sigler, P. B. (1994) The crystal structure of the bacterial chaperonin at 2.8 Å, *Nature* **371,** 578–582.

Brown, G. M., Noe-Spirlet, M. R., Busing, W. R., and Levy, H. A. (1977) Dodecatungstophosphoric acid hexahydrate $(H_5O_2^+)_3(PW_{12}\ O_{40}^{-3})$. The true structure of Keggin's pentahydrate' from single-crystal X-ray and neutron diffraction data, *Acta Crystallogr. Sect. B* **33,** 1038–1046.

Collaborative Computational Project No. 4 (CCP4) (1994) The CCP4 suite: Programs for protein crystallography, *Acta Crystallogr. Sect. D* **50,** 760–763.

Dawson, B. (1953) The structure of the 9(18)-heteropoly anion in potassium 9(18)-tungstophosphate, $K_6(P_2W_{18})O_{62})14H_2O$, *Acta Crystallogr.* **6,** 113–126.

Deisenhofer, J., Epp, O., Miki, K., Huber, R., and Michel, H. (1984) X-ray structure analysis of a membrane protein complex. Electron density map at 3 Å resolution and a model of the chromophors of the photosynthetic reaction center from rhodopseudomonos viridis, *J. Mol. Biol.* **180,** 385–398.

Frank, F., Zhu, J., Penczek, P., Li, Y., Srivastava, S., Verschoor, A., Radermacher, M., Grassucci, R., Lata, A. R., and Agrawal, R. K. (1995) A model of protein synthesis based on cryo electron microscopy of the *E. coli* ribosome, *Nature* **376,** 441–444.

Gabashivili, I. S., Agrawal, R. K., Grassucci, R., and Frank, J. (1999) Structure and structural variations of the *E. coli* 30S ribosomal subunit as revealed by three-dimensional cryo-electron microscopy, *J. Mol. Biol.* **286,** 1285–1291.

Goldgur, Y., Mosyak, L., Reshnetnikova, L., Anikolova, V., Lavrik, O., Khodyreva, S., and Safro, M. (1997) The crystal structure of phenylalanyl-tRNA synthetase from *Thermus thermophilus* complexed with cognate tRNA, *Structure* **5,** 59–69.

Harder, K., and Preetz, W. (1990) Schwingungsspektren der Clusterverbindungen, *Z. Anorg. Chem.* **591,** 32–40.

Harms, J., Tocilj, A., Levin, I., Agmon, I., Kölln, I., Stark, H., van Heel, M., Cuff, M., Schlünzen, F., Bashan, A., Franceschi, F., and Yonath, A. (1999) Elucidating the medium resolution structure of ribosomal particles: An interplay between electron-cryo-microscopy and X-ray crystallography, *Structure,* in press.

Hofmann, K. A. (1900) Über das Marcarbid, *Ber. Chem. Ges.* **33**(1), 1330–1339.

Hogle, J. M., Chow, M., and Filman, D. J. (1985) Three-dimensional structure of polivirus at 2.9 Å resolution, *Science* **229,** 1358–1365.

Jahn, W. (1989a) Synthesis of water soluble undecagold cluster for specific labelling of proteins, *Z. Naturforsch.* **44b,** 1313–1322.

Jahn, W. (1989b) Synthesis of water soluble tetrairidium cluster for specific labelling of proteins, *Z. Naturforsch.* **44b,** 79–82.

Jones, T. A., Zhou, J.-Y., Cowan, S. W., and Kjeldgaard, M. (1991) Improved methods for building protein models in electron density maps and the location of errors in these models, *Acta Crystallogr. Sect. A* **47,** 110–119.

Knäblein, J., Neuefeind, T., Schneider, F., Bergner, A., Masserschmidt, A., Löwe, J., Steipe, B., and Huber, R. (1997) Ta_6Br_{14}, a tool for phase determination of large biological assemblies by X-ray crystallography, *J. Mol. Biol.* **270,** 1–7.

Krumbholz, S., Schlünzen, F., Harms, J., Bartels, H., Kölln, I., Knaack, K., Bennett, W. S., Bhanumoorthy, P., Hansen, H. A. S., Volkmann, N., Bashan, A., Levin, I., Tocilj, A., and Yonath, A. (1998) Ribosomal crystallography: Cryo protectants and cooling agents, *Periodicum Biologorum* **100,** S2, 119–125.

Ladenstein, R., Bacher, A., and Huber, R. (1987) Some observations of a correlation between the symmetry of heavy atom complexes and their binding sites on proteins, *J. Mol. Biol.* **195,** 751–753.

Löwe, J., Stock, D., Jap, B., Zwickl, P., Baumeister, W., and Huber, R. (1995) Crystal structure of the 20S proteosome from Archeon *T. acidophilum* at 3.4 Å resolution, *Science* **268,** 533–539.

Luger, K., Maeder, A. W., Richmond, R. K., Segent, D. F., and Richmond, T. J. (1997) Crystal structure of the nucleosome core particle at 2.8 Å resolution, *Nature* **389,** 251–260.

Moore, P. B., Capel, M. S., Kjeldgaard, M., and Engelman, D. M. (1985) A 19 protein map of the 30S ribosomal subunit of *E. coli*, *In* Hardesty B., and Kramer, G. (Eds.), Structure, Function and Genetics of Ribosomes pp. 87–100, Springer-Verlag, Heidelberg, New York.

Mueller, F., and Brimacombe, R. (1997) A new model of the three-dimensional folding of *E. coli* 16S ribosomal RNA. II. The RNA–protein interaction data, *J. Mol. Biol.* **271,** 524–544.

Nar, H., Huber, R., Meining, W., Schmid, C., Weinkauf, S., and Bacher, A. (1995) Atomic structure of GTP cyclohydrolase I, *Structure* **3,** 459–466.

Neuefeind, T., Bergner, A., Schneider, F., Masserschmidt, A., and Knäblein, J. (1997) The suitability of Ta_6Br_{14} for phasing in protein crystallography, *Biol. Chem.* **378,** 219–221.

O'Halloran, T. V., Lippard, S. J., Richmond, T. J., and Klug, A. (1987) Multiple heavy-atom reagents for macromolecular X-ray structure determination. Application to the nucleosome core particle, *J. Mol. Biol.* **194,** 705–712.

Otwinowski, Z. (1993) Data collection and processing *in* Proceedings of the CCP4 Study Weekend, pp. 56–62.

Reinemer, P., Dirr, H. W., Ladenstein, R., Schaeffer, J., Gallay, O., and Huber, R. (1991) The three dimensional structure of class II glutathione *S*-transferase in complex with glutathione sulfonate at 2.3 Å resolution, *EMBO J.* **10,** 1997–2005.

Richmond, T. J., Finch, J. T., Rushton, B., Rhodes, D., and Klug, A. (1984) Structure of the nucleosome core particle at 7 Å resolution, *Nature* **311,** 532–537.

Ros, R., Scrivanti, A., Albano, V. G., Braga, D., and Garlaschelli, L. (1986) Chemistry of tetrairidium carbonyl clusters, *J. Chem. Soc. Dalton Trans.,* 2411–2421.

Rossmann, M. G. (1995) Ab initio phase determination and phase extension using non-crystallographic symmetry, *Curr. Opin. Struct. Biol.* **5,** 650–655.

Sagi, I., Weinrich, V., Levin, I., Glotz, C., Laschever, M., Melamud, M., Franceschi, F., Weinstein, S., and Yonath, A. (1995) Crystallography of ribosomes: Attempts at decorating the ribosomal surface, *Biophys. J.* **55,** 31–41.

Schlünzen, F., Hansen, H. A. S., Thygesen, J., Bennett, W. S., Volkmann, N., Levin, I., Harms, J., Bartels, H., Bashan, A.,

Berkovitch-Yellin, Z., Sagi, I., Franceschi, F., Krumbholz, S., Geva, M., Weinstein, S., Agmon, I., Boeddeker, N., Morlang, S., Sharon, R., Dribin, A., Peretz, M., Weinrich, V., and Yonath, A. (1995) A milestone in ribosomal crystallography: The construction of preliminary electron density maps at intermediate resolution, *J. Biochem. Cell Biol.,* **73,** 739–749.

Schneider, G., and Lindqvist, Y. (1994) Ta_6Cl_{14} is a useful cluster compound for isomorphous replacement in protein crystallography, *Acta Crystallogr. Sect. D* **50,** 186–191.

Stark, H., Mueller, F., Orlova, E. V., Schatz, M., Dube, P., Erdemir, T., Zemlin, F., Brimacombe, R., and van Heel, M. (1995) The 70S *E. coli* ribosome at 23 Å resolution: Fitting the ribosomal RNA, *Structure* **3,** 815–821.

Steipe, B., Pluckun, A., and Huber, R. (1992) Refined crystal structure of a recombinant immunoglobulin domain and a complementary-determining region 1-grafted mutant, *J. Mol. Biol.* **255,** 739–753.

Stöffler, G., and Stöffler-Meilicke, M. (1986). Immuno electron microscopy on *E. coli* ribosomes, *in* Hardesty B. and Kramer, G. (Eds.), Structure, Function and Genetics of Ribosomes pp. 28–46, Springer-Verlag, Heidelberg, New York.

Thygesen, J., Weinstein, S., Franceschi, F., and Yonath, A. (1996) On the suitability of multi metal clusters for phasing in crystallography of large macromolecular assemblies, *Structure* **4,** 513–518.

Volkmann, N., Hottentrager, S., Hansen, H. A. S., Zaytzev-Bashan, A., Sharon, R., Berkovitch-Yellin, Z., Yonath, A., and Wittmann, H. G. (1990) Characterization and preliminary crystallographic studies on large ribosomal subunits from *Thermus thermophilus, J. Mol. Biol.* **216,** 239–243.

von Böhlen, K., Makowski, I., Hansen, H. A. S., Bartels, H., Berkovitch-Yellin, Z., Zaytzev-Bashan, A., Meyer, S., Paulke, C., Franceschi, F., and Yonath, A. (1991) Characterization and preliminary attempts for derivatization of crystals of large ribosomal subunits from *Haloarcula marismortui,* diffracting to 3 Å resolution, *J. Mol. Biol.* **222,** 1–15.

Wada, T., Yamazaki, T., Kuramitsu, S., and Kyogoku, Y. (1999) Cloning of the RNA polymerase alfa subunit gene from *Thermus thermophilus* HB8 and characterization of the protein, *J. Biochem.* **125,** 143–150.

Weaver, T. M., Levitt, D. G., Donnelly, M. I., Wilkens, P., Stevens, P., and Banaszak, L. J. (1994) The multisubunit active site of fumarase C from *E. coli, Nat. Struct. Biol.* **2,** 654–662.

Wei, X., Dickman, M. H., and Pope, M. T. (1997) New routes for multiple derivatization of polyoxometalates: Diacetato-dirhodium-11-tungstophosphate, *Inorg. Chem.* **36,** 130–131.

Weinstein, S., Jahn, W., Hansen, H. A. S., Wittmann, H. G., and Yonath, A. (1989) Novel procedures of derivatization of ribosomes for crystallographic studies, *J. Biol. Chem.* **264,** 19138–19142.

Weinstein, S., Jahn, W., Laschever, M., Arad, T., Tichelaar, W., Haider, M., Glotz, C., Boeckh, T., Berkovitch-Yellin, Z., Franceschi, F., and Yonath, A. (1992) Derivatization of ribosomes and of tRNA with an undecagold cluster: Crystallographic and functional studies, *J. Crystal Growth* **122,** 286–292.

Xin, F., and Pope, M. T. (1994) Polyoxometalate derivatives with multiple organic groups. 1. Synthesis and structure of tris(organotin) beta-keggin and alpha-Dawson tungstophosphates, *Organometallic* **13,** 4881–4886.

Yan, Y., Stehle, T., Liddington, R. C., Zhao, H., and Harrison, S. C. (1995) Structure determination of simian virus 40 and murine polyomavirus by a combination of 30-fold and 5-fold electron density averaging, *Structure* **4,** 157–164.

Yonath, A., Glotz, C., Gewitz, H. S., Bartels, K., von Boehlen, K., Makowski, I., and Wittmann, H. G. (1988) Characterization of crystals of small ribosomal subunits, *J. Mol. Biol.* **203,** 831–833.

Yonath, A., and Franceschi, F. (1998) Functional universality and evolutionary diversity: Insights from the structure of the ribosome, *Structure* **6,** 678–684.

Yonath, A., Harms, J., Hansen, H. A. S., Bashan, A., Peretz, M., Bartels, H., Schluenzen, F., Koelln, I., Bennett, W. S., Levin, I., Krumbholz, S., Tocilj, A., Weinstein, S., Agmon, I., Piolleti, M., Auerbach, T., and Franceschi, F. (1998) The quest for the molecular structure of a large macromolecular assembly exhibiting severe non-isomorphism, extreme beam sensitivity and no internal symmetry. *Acta Crystallogr. Sect.* **54,** 945–955.